Mesoscale Precipitation Patterns in an Occluded Frontal System

Shinn-liang Shieh

Central Weather Bureau, Taipei, Taiwan, ROC

(*Manuscript received 15 March 1976, in revised form 30 March 1976*)

Abstract

A case study is presented which illustrates the characteristics and behavior of mesoscale precipitation features associated with an occluded frontal system passing through western Washington State. During the storm period (December 5-7, 1973), six rainbands were observed by means of autographic raingauge and radar data. The first five bands were similar in size, about 50 km in width on average, while the width of the last band was 100 km. The first two bands, observed on December 5, appeared to have been parallel to the warm front of the occluded system. The next two bands, observed on December 6, occurred in the warm sector of a wave which had developed on the cold front and were probably parallel to the cold front. These two bands moved from the southwest at about 35 km h^{-1}. The final two bands, observed on December 7, were parallel to the cold front and accompanied its passage. Smaller scale elements, with mean sizes of 50 –240 km^2, were embedded in the rainbands in concentrations of 1 to 3 per 1000 km^2 and they moved with the wind between 850 and 700 mb (presumably the levels where precipitation particles were generated). The vertical extent of all of the mesoscale rain areas was estimated to be between 3 and 7 km.

1. Introduction

In recent years, several studies of the mesoscale structure of precipitation in extra-tropical cyclones have been presented. Some of these investigations have revealed the existence of rainbans on the order of 50 km in width and hundreds of kilometers in length within frontal cloud systems. Elliott and Hovind (1964), in a study of Pacific fronts in California, found that organized convective bands were frequently embedded in the large-scale precipitation region of the storm. Browning and Harrold (1969) analyzed a wave depression over the British Isles in great detail. They showed that bands of heavy rain occurred parallel to and ahead of warm front. Kreitzberg and Brown (1970) in studying mesoscale weather systems within an occlusion also found that the convection is aligned in bands roughly parallel to the wind shear in the convective layer. Houze (1969) and Austin and Houze (1970, 1972) examined seventeen cyclones over New England. They found that precipitation areas on the sub-synoptic scale with rather clearly

definable characteristics and behavior were contained in all storms. They classified the subsynoptic-scale precipitation areas into three categories: (1) *large mesoscale areas* which ranged from 10^3-10^4 km^2 in area, (2) *small mesoscale areas* which covered 100-400 km^2, and (3) *cells*, roughly 10 km^2 in area (cumulus-scale), which were located within the small mesoscale areas. Some of the large mesoscales were definitely bandshaped. Reed (1972) in a continuation of Austin and Houze's work found that the larger bands ($\sim 10^4$ km^2 in area) ahead of cyclones were systematically parallel to the warm front and moved in the same direction as the warm front, but slightly faster.

The relation of the movement of the small mesoscale rain areas to the upper-level winds has been discussed by several investigators. For example, Browning and Harrold (1969), Austin and Houze (1972), and Harrold (1973) observed that the motion of small mesoscale rain areas is controlled by the wind at a height of 3-6 km (about 700 to 500 mb).

The purpose of the present study was to obtain a better understanding of the nature and behavior of mesoscale* precipitation patterns associated with an occluded frontal system which passed through western Washington during December 5-7, 1973. The raingauge and radar data mentioned above were examined to identify sub-synoptic features of the precipitation pattern in the frontal case selected for study. The size, concentration and motions of the identified features have been determined and related to larger-scale features of the parent frontal system.

2. Field Observations

Data for this study were obtained from various field sites in western Washington State during December 5-7, 1973. The locations of these sitesand the types of data collected are shown in Fig. 1.

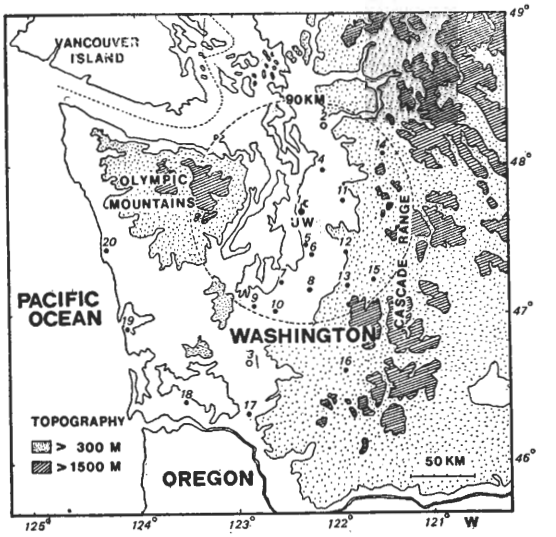

Fig. 1. Locations of field stations and types of data collected. Symbols indicate types of data as follows: ◦ --high-resolution raingauge, • --low-resolution raingauge, ⨍ --The University of Washington radars and rawinsonde. Approximate radar range for the University of Washington is enclosed by dashed circle. Raingauge stations are indicated: (1) University of Washington, (2) Arlington, (3) Chehalis, (4) Evertt, (5) Seattle-Tacoma Airport, (6) Auburn, (7) McChord Air Force Base, (8) McMillin Reservoir, (9) Olympia, (10) Yelm, (11) Carnation, (12) Landsberg, (13) Mud Mountain Dam, (14) Silverton, (15) Greenwater, (16) Randle, (17) Castle Rock, (18) Grays River, (19) Westport, (20) Point Grenville.

2.1 Raingauge Data

The high-resolution raingauges, shown at three sites in Fig. 1. were tipping-bucket

*The term mesoscale in this thesis refers to identifiable precipitation features with horizontal areas of the order of 10^2 to 10^4 km^2 in area.

gauges operated by the University of Washington; each has a resolution of approximately 0.04 mm of rain per tip. The time resolution of these gauges was about 15 sec. in moderate rain. The low resolution gauges, located as shown in Fig. 1, were weighing-bucket ganges operated by the National Weather Service. From these gauges, rainfall amounts of approximately 0.5 mm could be resolved over time periods as short as 7 min.

2.2 Radar Data

Two radars were operated at the University of Washington. One was a weather surveillance radar which provided approximately horizontal coverage within a 90-km radius of the University of Washington (see Fig. 1). The other was a vertically-pointing pulsed Doppler radar which detected precipitation and the spectrum of particle fallspeeds at ten heights. A complete set of Doppler radar data in the vertical was obtained at intervals of 50 sec. The characteristics of the two University of Washington radars are listed in Table 1.

Table 1. Characteristics of the University of Washington Radars.

	Surveillance Radar	Doppler Radar
Wavelength	3.2cm	3.2cm
Beamwidth	1°	2.8°
Peak Power	250KW	7KW

The PPI (plan position indicator) displays from the surveillance radar were cycled through five gain settings (referred to below as levels 0 to 4; the most sensitive one is level 0.) and recorded in a time-lapse fashion on 16-mm motion picture film. The Doppler radar data were recorded both digitally and photographically.

2.3 Other Data

Other types of data referred to in this study include satellite photographs and conventional weather data obtained from National Environmental Satellite Service and the National Weather Service. This information was supplemented by serial rawinsondes launched at two to three hour intervals from the University of Washington.

3. Frontal System of December 5-7, 1973

3.1 Synoptic Situation

At 0400 PST (Pacific Standard Time) on December 5, 1973, a deep cyclone in the North Pacific was centered at 49°N, 143°W, approximately 1,500 km to the west of Seattle (Fig. 2). An occluded frontal system extended southward from the cyclone center. The surface cyclone and front were associated with a 500-mb trough, centered on 150°W. The movements of the surface cyclonic system are illustrated in Fig. 3. The surface front progressed eastward at an average speed of about 45 km h^{-1}. It slowed down considerably as it approached the coastline of the United States and Canada. At 1000 PST on December 6 a wave developed along the surface front to the south of Vancouver Island and then moved across the island toward the northeast (Fig. 3)*. On the morning of December 7 the frontal system passed over Seattle.

*The frontal positions shown in Fig. 3 were obtained from a University of Washington synoptic laboratory class in which the frontal positions were derived at a classroom exercise. These positions do not differ greatly from the National Weather Service's analysis of the same situation.

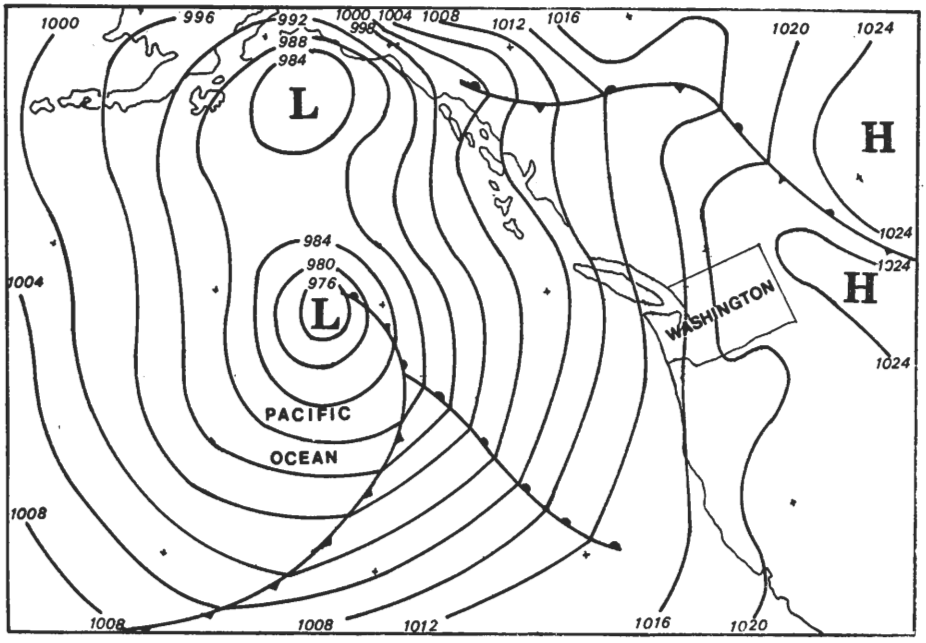

Fig. 2. Surface map for 0400 PST December 5, 1973. Isobars labelled in millibars. Small crosses are intersections of latitude and longitude lines on base map at intervals of 10°

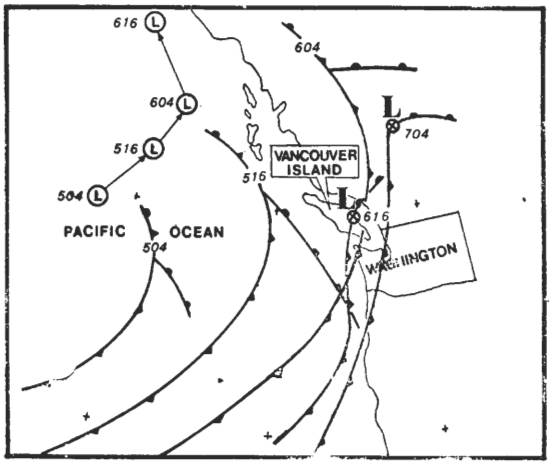

Fig. 3. The movements of surface cyclonic and frontal systems during December 5-7, 1973. First digit of numbers gives date of day followed by hours in Pacific Standard Time.

The progression of the frontal clouds over the eastern Pacific Ocean and northwestern United States may be seen in the sequence of satellite photographs in Fig. 4. At 2200 PST on December 4, the leading edge of the frontal clouds was located along 135°W between 40°N and 50°N (Fig. 4a). During the next 36h, the cloud system moved over the northwestern coastline of the United States (Figs. 4b-d). At 2200 PST on December 6, the frontal wave development south of Vancouver Island manifested itself as a bulge in the frontal cloud band (centered near 45°N and 127°W in Fig. 4e). By 1000 PST on December 7 the frontal cloud system had passed over western Washington State (Fig. 4f).

From the serial rawinsonde data collected at the University of Washington (UW), Department of Atmospheric Sciences, vertical time-sections of relative humidity, and wet-bulb potential temperature (θ_w) over the UW were constructed (Fig. 5). The frontal symbol shown aloft on December 5 indicates the core of a θ_w maximum (Fig. 5b) preceeding a cool, dry period aloft, however, neither synoptic maps nor satellite pictures establish its identity as a true front. Interestingly, barograph traces showed a trough passing over the UW at 1600 PST on the fifth coinciding with the passage of this weak "front" aloft.

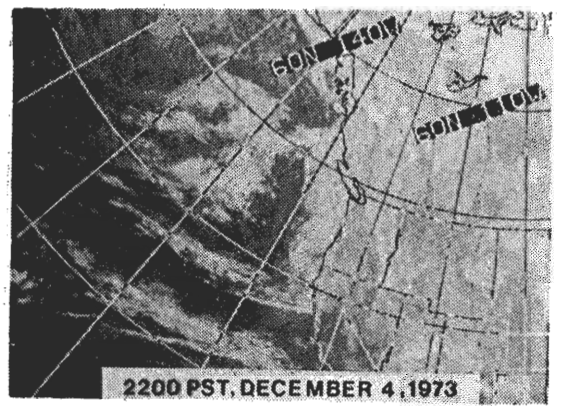

(a)

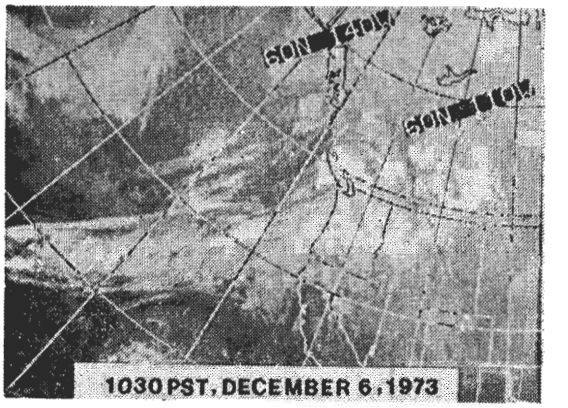

(d)

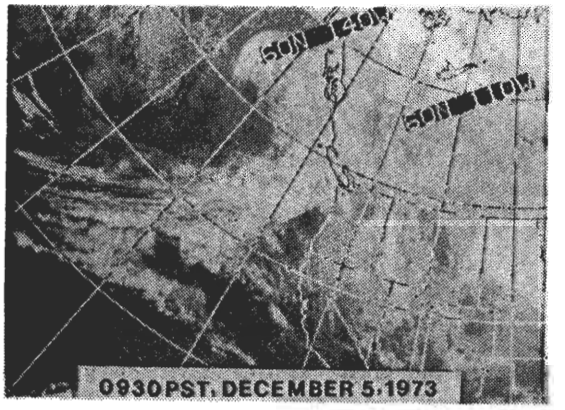

(b)

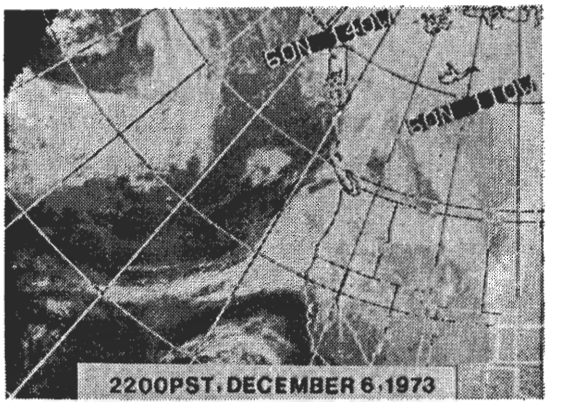

(e)

(c)

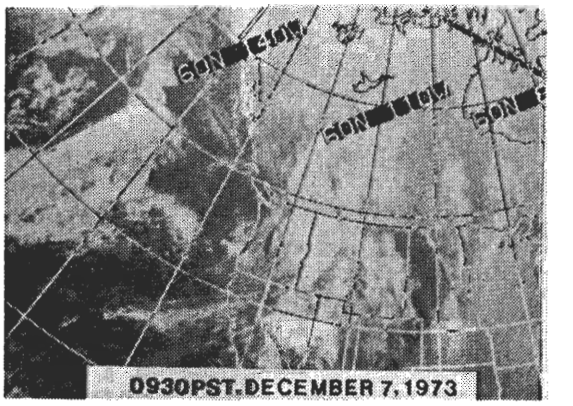

(f)

Fig. 4. NOAA-2 satellite infrared mosaics for December 5-7, 1973. Beginning time of passing over Washington State area is indicated for each mosaic. Intervals between latitude lines are 10°

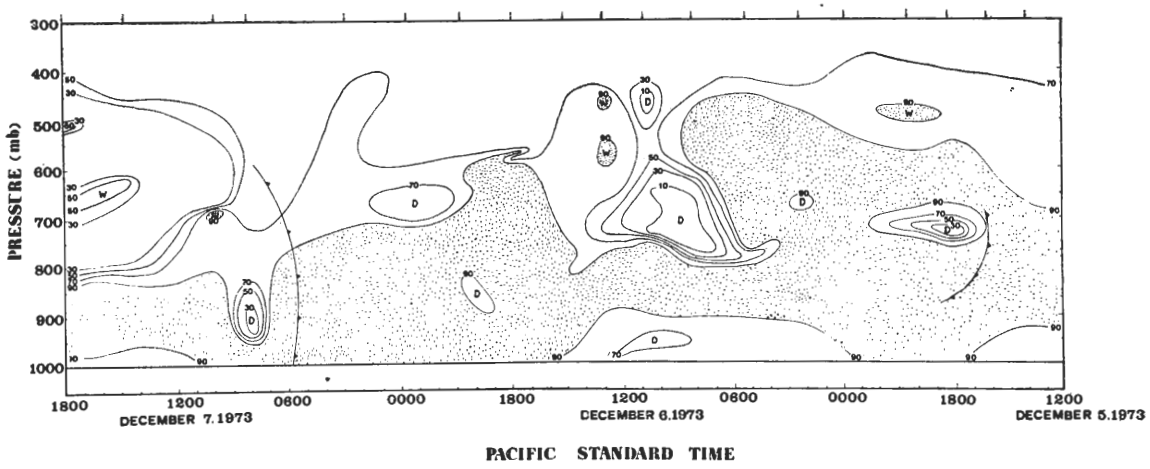

Fig. 5(a). Time-height section of relative humidity (in %) at the UW. Stippled areas indicate relative humidity over 90%.

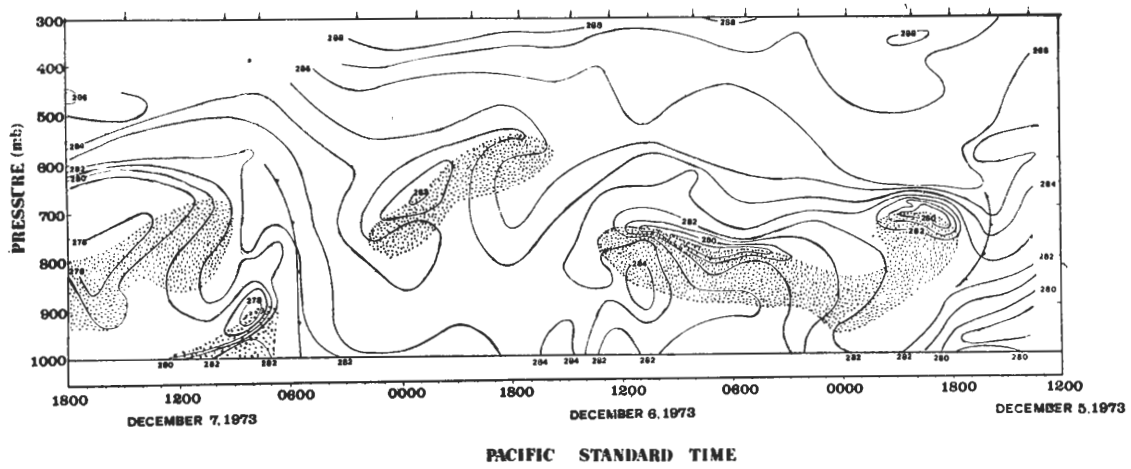

Fig. 5(b). Time-height section of wet-bulb potential temperature (θ_w in °K) at the UW. Stippled areas denote potential instability.

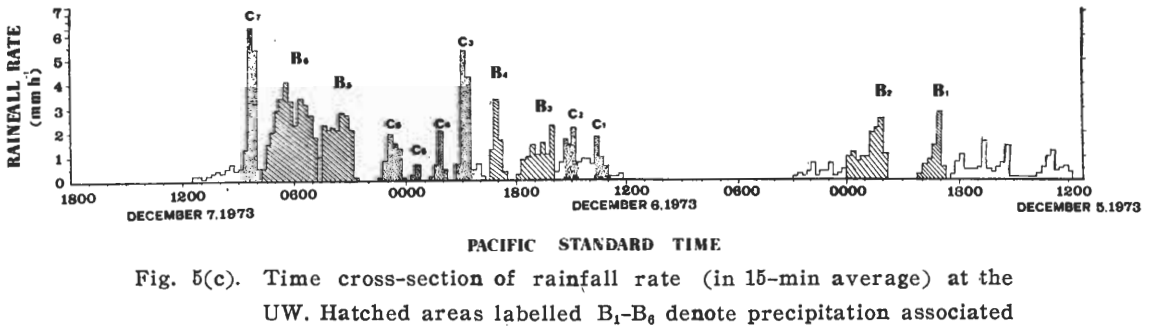

Fig. 5(c). Time cross-section of rainfall rate (in 15-min average) at the UW. Hatched areas labelled B_1-B_6 denote precipitation associated rainbands B_1-B_6, and stippled areas labelled C_1-C_7 indicate precipitation associated with non-band rainfall elements.

15-min average rainfall rates at the UW are shown in Fig. 5c. The variation of precipitation intensity with time is quite irregular which suggests that the precipitation was controlled by processes on the sub-synoptic scale. It is noteworthy that during the period of no precipitation on December 6, a significant core of low relative humidity appeared over the UW and cores of dry air were also observed right after the frontal passages.

In Fig. 5b, the stippled areas denote potential instability. In comapring Figs. 5a, b, and d, it is seen that the potentially unstable air over the UW was generally associated with regions of dry air aloft and had no significant correlation with periods of rainfall. Only the peak labelled C_7 in Fig. 5c occurred during a definitely potentially unstable* period. Note the prominent decrease of θ_w with height below the 900-mb level coinciding with C_7 in Fig. 5b and c. Convection in C_7 apparently penetrated the dry air aloft which was detected by the soundings. Most other peaks occurred when potential instability was weak or nearly in a neutral condition and appeared to be embedded in a generally moist layer aloft. This suggests that embedded convection may have already been taking place and the associated vertical mixing had eliminated the vertical gradient of θw in these regions.

3.2 Precipitation Stucture

3.2.1 Method of Locating Rainbands

An analysis of the raingauge data from all of the stations in Fig. 1 was undertaken to determine if any of the subsynoptic-scale peaks in rainfall rate observed at the UW (Fig. 5c) could be explained by the systematic movement of rainfall rate patterns from station to station. The rainfall periods indicated by shading and the notation B_1–B_6 in Fig. 5c were found to be associated with mesoscale rainbands embedded within the synoptic-scale weather system. Each of these large rainbands could be tracked for at least four hours, from the time it appeared over the Washington coast until it move into the Cascade Mountains in central Washington. The rainfall maxima labelled C_1–C_7 in Fig. 5c were generally too small to be tracked from raingauge to raingauge because of the large spacing between stations. However, these small areas were observed on radar.

The procedure for following the rainbands, B_1–B_6, from station to station involved first plotting the 15-min average rainfall rates for all the gauge stations. The resulting plots were then arranged in order of their geographical situation, and similarities in the time distributions of rainfall rates were noted and labelled, as shown for bands B_1 and B_2 in Fig. 6.

The times that the front and back edges of each feature passed over each station were plotted on a horizontal map and isochrones of the front and back edges were constructed. From the isochrone patterns, the positions of the rainbands were constructed. Elliott and Hovind (1964) used a method similar to the one described here to locate mesoscale rainbands within the general rain areas of Pacific frontal systems moving into California.

In comparing raingauge traces such as those shown in Fig. 6 there is some subjectivity involved in deciding on the boundaries of features such as B_1 and B_2. The chosen boundaries were checked in two ways. First, it was assumed that the large bands moved in a more or less continuous manner over the raingauges, therefore, the boundaries were required to produce reasonably

*Potential instability refers to a decrease of θ_w with height.

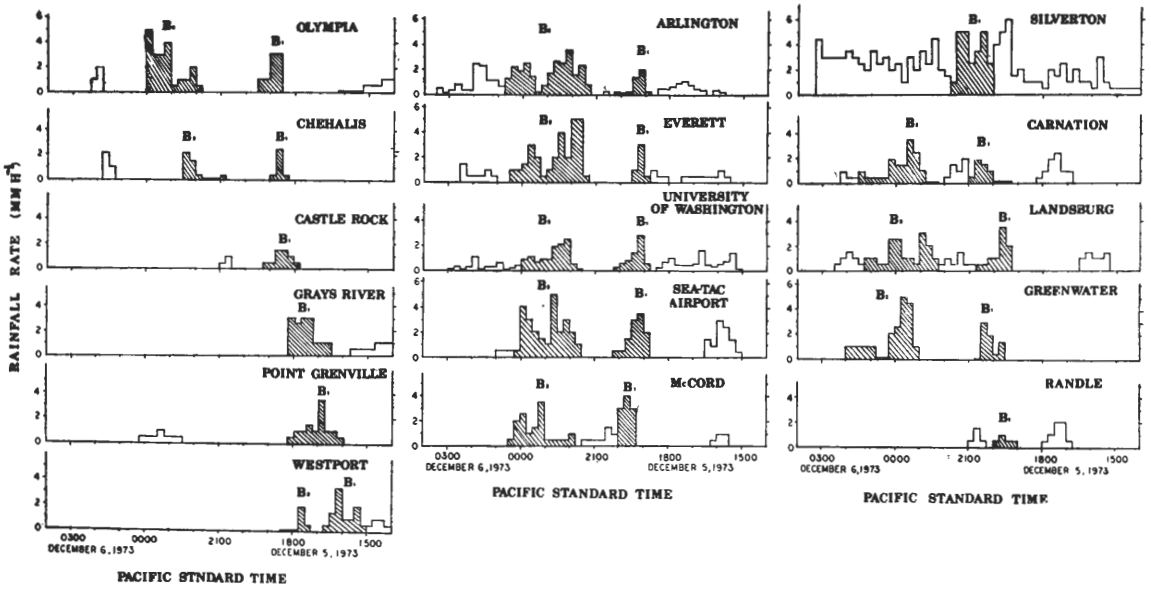

Fig. 6. Fifteen-minute average rainfall rates for stations in western Washington. Hatched regions indicate passages of rainbands B_1 and B_2.

continuous isochrone patterns for both front and back edges. Second, the weather surveillance radar data were utilized to check the band structure deduced from the gauge data whenever the bands were in radar range.

3.2.2 General Feature of Rainbands

Fig. 7 Shows an example of the positions of rainbands B_1 and B_2 at selected time Rain echoes observed on the surveillance weather radar operated at the UW are superimposed on the positions of bands which were in radar range.

Characterestic features of the six rainbands B_1-B_6 mentioned above are summarized in Table 2. It can be seen from Table 2 that B_1-B_5 were very similar in size, and rainfall intensity, while B_6 was much larger in size, more intense in rainfall rate, and produced more precipitation at a station. Band B_6 which coincided with the primary cold front had a mean width of about 100 km which is about the same dimension as the dominant rainbands which were oriented parallel to the surface cold front in a case studied by Browning et al. (1973)

Table 2. Characteristics of rainbands observed on December 5-7, 1973. Numbers in parentheses are extremes. Direction in degrees are those from which the rainbands moved.

Rainband	Period of observation (PST)	Number of stations passed over	Mean rainfall rate (mm h^{-1})	Maximum rainfall rate (mmh^{-1})	Mean duration over a station (min)	Mean amount of rain at a station (mm)	Width (km)	Orientation (relative to true north)	Velocity normal to band orientation (km h^{-1})
B^1	1500-2130 December 5	17	1.5 (0.4-4.3)	5.1	80 (45-135)	2.0 (0 6-5.3)	47 (28-80)	N-S	47/250°
B^2	1715-0020 December 5	13	1.6 (0.5-3.2)	5.1	160 (75-210)	4.4 (0.4-9.7)	43 (23-100)	N-S to NNW-SSE	26/260°
B^3	1045-2000 December 6	18	1.6 (0 2-3.9)	8.2	120 (45-195)	3.2 (0.2-7.0)	65 (40-85)	NW-SE	30/220°
B_4	1300-2200 December 6	11	1.6 (0.3-3.8)	8.1	90 (45-150)	2.6 (0.6-10.3)	45 (25-68)	WNW-ESE to NW-SE	38/230°
B_5	2215-0500 December 6-7	13	1.7 (0.2-3.1)	5.1	90 (15-165)	2.5 (0.2-4.6)	40 (30-52)	N-S to NNW-SSE	27/260°
B_6	0115-0515 December 7	20	3.6 (1.8-5.7)	13.7	180 (135-225)	14.1 (5.5-21.2)	100 (90-110)	N-S	36/265°

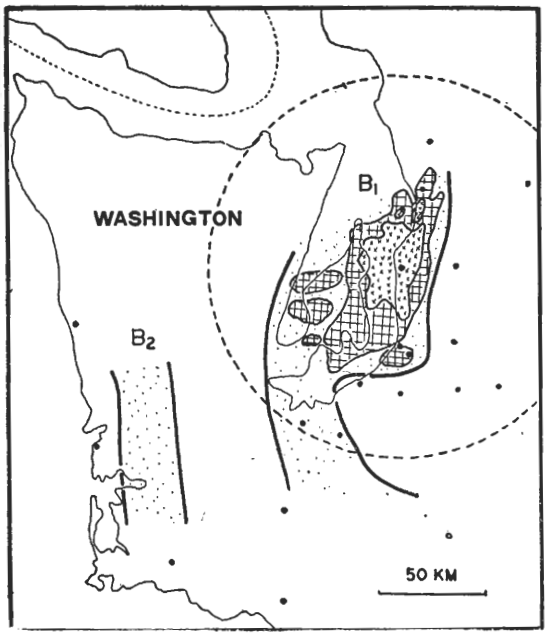

Fig. 7. Position of two rainbands B_1 and B_2 at 1900 PST December 5, 1973.
▨ : rainband.
▦ : precipitation area as seen by radar at the highest gain setting (level-0).
▩ : precipitation core as seen by radar at the lowest gain setting (level-4).

The rainbands during the storm period of December 5-7, 1973, could be grouped by orientation. Rainbands B_1, B_2, B_5, and B_6 were all approximately oriented in north-south direction and progressed eastward across the observational network, while B_3 and B_4 were oriented southeast-northwest and moved from the southwest. The relationship of the band orientations to the large-scale frontal system and its associated cloud shield can be seen in Fig. 8. From Fig. 8a, it can be seen that bands B_1 and B_2 were located toward the leading edge of the cloud shield, and B_1 and B_2, being oriented north-south, would have to be rotated counterclockwise through an angle of 20 to 30° to become parallel to the cold front at the trailing edge of the cloud shield. Kreitzbergand Brown (1970) found rainbands oriented in a similar sense relative to the surface front within the leading section of an occluded cloud system. They found further that in the middle region of the cloud shield the rainband orientations veered sharply and were parallel to the cold front on the trailing side of the system.

From Fig. 3, it can be seen that after 1900 PST on December 5 (the time of Fig. 8a) the cold front moved toward the Washington Coast and stalled just offshore until early morning on December 7. The warm front, originally analyzed over the ocean on December 5, had apparently moved northeastward into western Cascade, north of Vancouver Island, and lost its identity after 0400 PST on December 6. By 1600 PST, on December 6, the time which rainbands B_3 and B_4 were passing over Washington, a frontal wave cyclone had appeared and distorted the previous cold front. In Fig. 8b two analyses are shown. The frontal positions shown by solid lines are those from Fig. 3 and were determined by the synoptic laboratory class, as the footnote explained in § 3.1. According to the class analysis in Fig. 8b, B_3 and B_4 do not appear to be parallel to either the cold front or the warm front associated with the frontal wave. The frontal positions over the ocean, however, are by no means certain, and the fronts could be reanalyzed as shown by the dashed lines in Fig. 8b. In fact the reanalysis is supported by the ship wind report included in Fig. 8b. There is, of course, no conclusive evidence regarding the frontal positions at the time of Fig. 8b. The purpose of the reanalysis is to show that B_3 and B_4, located in the warm sector of the wave, could have been parallel to the cold front and that the orientation of B_3 and B_4 is therefore not necessarily inconsistent with the result of Nozumi and Arakawa (1968) who found that warm sector bands almost always occur in oceanic cyclones near Japan

and that the bands tend to be parallel to the cold front. Nor are the present results inconsistent with those of Elliott and Hovind (1964), Kreitzberg and Brown (1970), and Harrold (1974) who have consistently found bands to be parallel to the wind shear aloft, in layers containing the precipitating clouds.

Bands B_5 and B_6, shown in Fig. 8c, were obviously parallel to the surface cold front.

A noteworthy common feature of all six bands (B_1-B_6) as they moved into the Puget Sound Basin was that their bandwidths became enlarged and they rotated slightly in their orientation (B_1, B_2, clockwise, B_3, B_4, B_5, B_6, counterclockwise). This is possibly due to effects of topography.

3.2.3 Small-scale Elementsin Rainbands

In an attempt to gain further insight into the horizontal structure of the rainbands discussed in the previous section, the UW radar data were examined. The data were used to evaluate the concentrations, mean sizes, and horizontal motions of rain areas which were embedded in the different rainbands. Table 3 lists the properties of sampled radar echoes within each rainband.

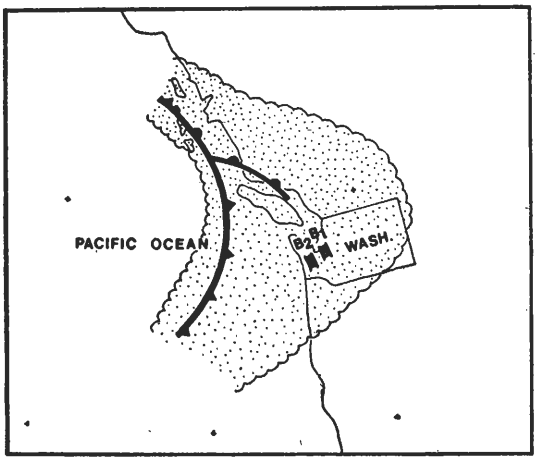

(a)

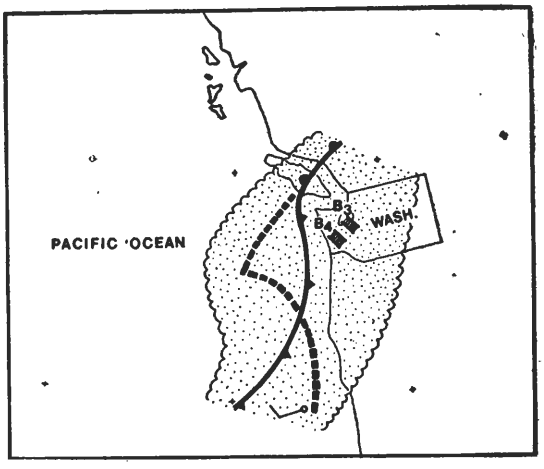

(b)

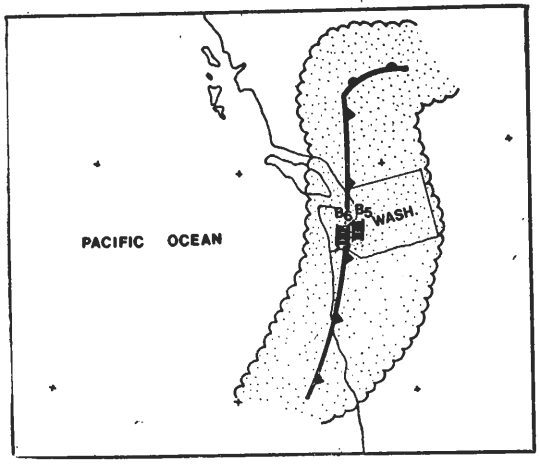

(c)

Fig. 8 (a-c). Surface fronts (from class analysis, see footnote in p.14), cloud shield (estimated from satellite observations), and rainbands at three times.

(a) Bands B_1 and B_2 at 1900 PST on December 5.

(b) Bands B_3 and B_4 at 1000 PST on December 6.

(c) Bands B_5 and B_6 at 0400 PST on December 7.

In (b) dashed lines show reanalysis of surface fronts for this time. Wind vector is shown for a key ship report used in the reanalysis.

Table 3. Properties of small-scale rain echoes sampled at the highest (level-0) and lowest (level-4) radar gain settings within the rainbands B_1-B_6. Direcions in degrees are those from which the radar echoes moved. Numbers in parentheses are extremes.

Level-0

Rain-band	Average number of separate echoes per 1000 km²	Average area of echoes (km²)	Average velocity of echo (km h⁻¹)
B_1	1.3	344(118-585)	78/220°
B_2	1.5	295(71-537)	78/220°
B_3	1.3	267(58-635)	85/215°
B_4	1.8	173(18-500)	90/210°
B_5	2.8	200(49-440)	80/215°
B_6	1.5	65(45-120)	70/215°

Level-4

Rain-band	Average number of separate echoes per 1000 km²	Average area of echoes (km²)	Average velocity of echo (km h⁻¹)
B_1	1.1	91(43-170)	80/225°
B_2	1.7	50(10-202)	96/225°
B_3	0.7	47(20-100)	100/210°
B_4	0.8	23(20-25)	88/205°
B_5	0.9	34(18-100)	80/215°
B_6	1.1	48(23-90)	60/225°

It can be seen from Table 3 that the dimensions of the mean echo sizes at two different radar gain settings (i.e. level-0 and level-4) were on the order of approximately 10 to 100 km², respectively. Similar features in precipitation echo patterns have also been observed in storms in other geographical area, e.g. Austin and Houze (1972).

Table 3 also shows that the mean concentration of echoes at the highest gain (level-0) in every 1000 km² area of a rainband was almost the same in bands B_1-B_5, with slightly higher value in B_6. These concentrations (1-3 per 1000 km²) are very close to the values of the average density of SMSA's evaluated by Houze (1969) and Austin and Houze (1972) in New England. Their average concentration of SMSA's was about 1.3 in every 1000km² area. The mean concentration of echoes at the lowest gain (level-4) of the six rainbands B_1-B_6 was about 1.1 per 1000 km² area. However, Houze (1969) found that the average density of cells in each LMSA was approximately 4.0 per 1000 km² area which is slightly higher than the value obtained in this case study.

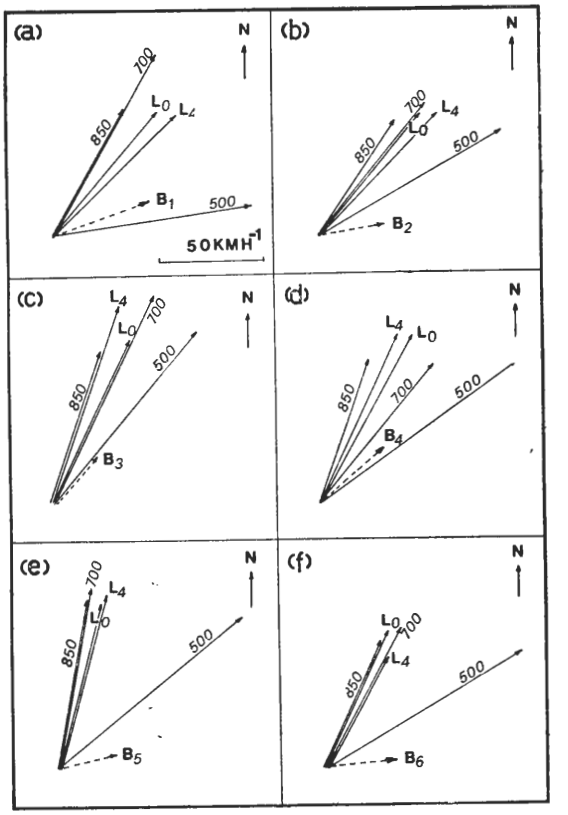

Fig. 9. Schematic diagram showing the relation of motion of rainbands to their embedded small-scale echoes and to the winds at 850, 700, and 500 mb level. Arrows labelled L_0 and L_4 denote the mean velocity of small-scale echoes at the lowest and the highest intensity level, respectively, and B_1-B_6 indicate the component of rainband velocity normal to its orientation. and 850, 700 and 500 represent mean wind velocity at 850, 700, and 500 mb level, respectively.

The mean velocity vectors of the lowest and the highest rainfall intensity echoes (labelled L_0 and L_4 in Fig. 9) within the rainbands B_1-B_6 were compared with the mean upper winds (see Fig. 9). The arrows labelled 850, 700 and 500 represent the winds at 850 700 and 500 mb level, respectively. The movement of echoes embedded in the rain band are the same as the wind directions at the 850 and 700 mb levels to within 15°. The level-0 and level-4 echo velocities are in close agreement in each rainband, and their agreement with the 850 and 700 mb wind velocities suggests that these small-scale elements were guided by the flow at these levels. From Fig. 9a-d, it is seen that the component of small-scale echo motion normal to the rainband (i.e. parallel to the dashed vector in each figure) was larger than that of the band itself (given by the magnitude of the dashed arrows). Thus, in bands B_1-B_4, the small-scale elements moved from the back toward the front edge of each band. This observation suggests that the motion of these large-scale bands was controlled by factors other than those controlling the small-scale element motion. The motion of the large bands may be related either to winds aloft or to the movement of the parent large-scale synoptic system. The component of small-scale echo motion normal to B_5 and B_6 is seen from Figs. 9e and f to be nearly equal to that of the band motion.

The "cells and SMSA's" in Austin and Houze's (1972) study moved with the wind at mid-cell height, which ranged from 700 to 500 mb. Rain areas of similar size, observed by Browning and Harrold (1969) and Harrold (1973), were controlled by the wind at a height of 3-6 km (or approximately 700 to 500 mb). The small-scale rain areas in any given case are probably steered by the winds in the layer where the precipitation is generated. In this case, that layer (850-700 mb) is slightly lower than in those cases analyzed by previous investigators.

3.2.4 Non-band Small-scale Rain Areas

In the previous sections we have mentioned that the irregular distribution of rainfall rate against time at the UW (Fig. 5c) was associated with subsynoptic-scale processes. In addition to the peak rainfall rates associated with the passage of the six bands labelled B_1-B_6, some other significant peaks occurred and are labelled C_1-C_7 in Fig. 5c. The first six peaks (C_1-C_6) were due to the contribution of individual mesoscale rain areas which passed over the UW but exhibited no obvious band shape and were generally too small to be detected by the raingauge network. These areas were, however, identified by further examination of the time lapse PPI sequence available during the storm period. Mesoscale areas C_1-C_6 all moved into the radar range from the southwest, at the entrance to the Puget Sound Basin, and progressed toward the northeast. Their characteristics are listed in Table 4. During the course of their motion as they approached the UW, each of the areas C_1-C_3 appeared first only at the highest gain setting (level-0), however, as the echo approached the UW, it appeared as an intense core at the lowest gain (level-4) embedded in a weaker level-0 echo.

From the data in Table 4, it seems that the motion of the small elements was closely correlated with the 850 mb and 700 mb winds aloft, as were the small-scale elements in the bands B_1-B_6 (see § 3.2.3). The duration of the mesoscale areas, C_1-C_6, passing over the U. W was in the range between 30 to 60 min, and the echoes were generally 60 km in horizontal dimension and their horizontal motion was from the southwest at 60 to 90 km h^{-1}. Thus, they correspond in size to the SMSA's observed by Austin and Houze (1972).

Table 4. Characteristics of non-band small-scale precipitation elements observed on the radar during December 6-7, 1973. Horizontal dimensions for C_1-C_6 were determined by multiplying their time of passage over the UW by the echo speed. Start and end times for C_1-C_6 were determined by extrapolating echo motions over the UW. Horizontal dimension for C_7 was determined from radar PPI photographs and its start and end times inferred from the appearance of the raingauge trace in Fig. 5c. Direction of echo velocities and upper winds are those from which echoes or air moved.

Small-scale non-band area	Radar intensity level	Mean velocity (km h^{-1})	Time at UW (PST)		Rainfall rate at UW(mmh^{-1})		Horizontal dimension over UW (km)	Upper winds (km h^{-1})		
			Start	End	Mean	Peak		850mb	700mb	500mb
C_1	0→4	80/215°	1255	1345	0.8	1.7	66	75/205°	75/210°	130/235°
C_2	0→4	90/215°	1435	1530	1.3	2.2	78	75/210°	110/215°	110/230°
C_3	0→4	60/235°	2025	2055	4.7	5.4	40	95/200°	90/210°	110/230°
C_4	0	70/220°	2200	2240	0.9	2.0	47	90/200°	9 /210°	120/230°
C_5	0	80/220°	2300	2330	0.4	0.6	40	90/205°	90/215°	120/235°
C_6	0	60/240°	000	0130	0.9	1.9	90	90/200°	75/210°	110/230°
C_7	4	0	0800	0845	4.4	6.4	50			

The maximum intensity peak, labelled C_7 in Fig. 5c, corresponds to an echo observed on the PPI scope which appeared to be stationary from the very beginning until it dissipated. This feature probably can be explained as the result of local convergence of the airflow in the vicinity of Seattle in the Puget Sound Basin which occurred right after the frontal passage and the release of potential instability over the UW (Fig. 5b) which was responsible for the convective nature of the mesoscale rain area C_7 observed on the morning of December 7, 1973.

Unfortunately, it was not possible to identify mesoscale rain areas which contributed to the peak intensities shown in Fig. 5c on December 5, 1973 (other than the bands B_1 and B_2) due to the lack of PPI photographs for this time period.

3.2.5 Vertical Structure of Rain Areas

A height-time section, utilizing data from the vertically pointing pulsed Doppler radar located at the UW, was constructed in order to relate the upper-level moisture features to the surface precipitation patterns (Fig. 10). Broadly speaking the vertical extent of echo detected by the Doppler radar (stippled areas in Fig. 10) correlated positively with the surface rainfall rate patterns (plotted along the abscissa in Fig. 10). It is seen that in most cases the vertical extent of the echoes reached above 4.3 km, however, due to the limitation of the available radar data in vertical extent, it is not possible to identify the maximum extent of the top of echoes. With a view to estimating the vertical extent of the echoes, the time-height section of relative humidity (Fig. 5a) was used for reference. A line labelled 70% (relative humidity with respective to liquid water) in Fig. 5a was chosen as the probable maximum upper bound of the vertical extent of the echoes. The 70% line on December 5, 1973, extended up to a height of 7 km, while on December 6 it reached a height of approximately 4-5 km, and on December 7 it varied from 3 to 7 km. As mention in §3.1 above, C_7 differed from the other areas (B_1-B_6 and C_1-C_6) by penetrating a dry layer aloft.

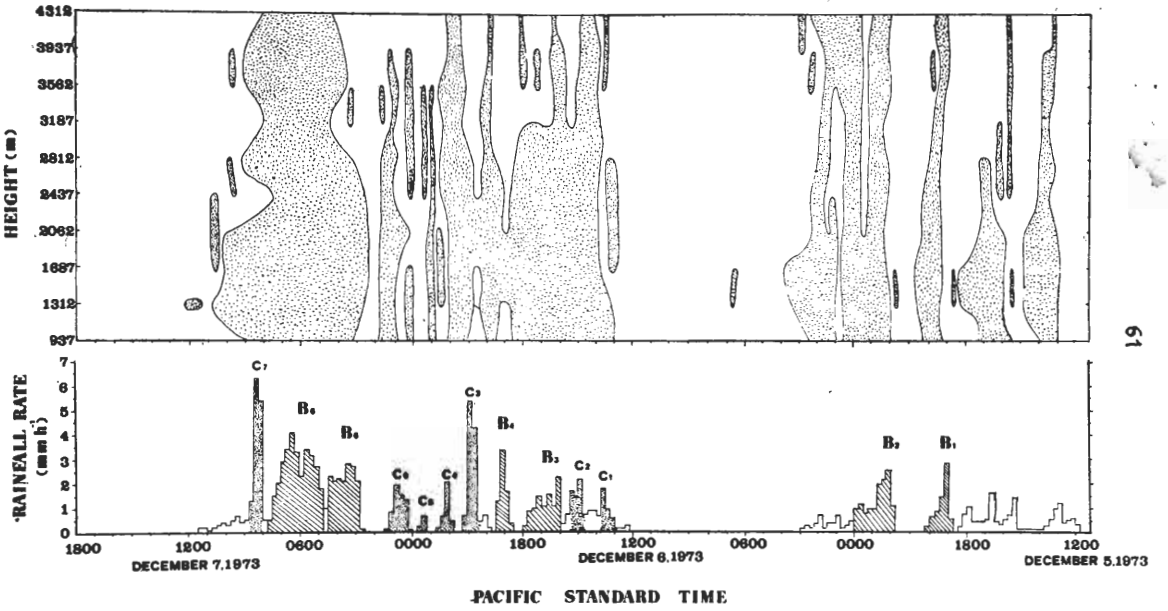

Fig. 10. Time-height section showing the vertical extent of the echo detected by the Doppler radar at the UW. The ten levels on the height scale correspond to the ten levels sampled by the radar. Contours were obtained by analyzing the data from these discrete levels.

Austin and Houze (1972) found that the average vertical extent of the cells and of surrounding precipitation in the cyclonic storms they studied were about 4–6 and 4–10 km, respectively. Browning and Harrold (1969) also found the vertical extent of echoes detected by the Doppler radar in vicinity of a front was 3–6 km. They are similar to the finding in this case study.

4. Conclusions

In this case study the characteristics and structure of mesoscale precipitation areas associated with an occluded frontal system which passed through western Washington State during December 5–7, 1973, have been described,

During this storm, six rainbands (B_1-B_6) which were identified with the aid of autographic raingauge data and a sequence of time-lapse radar PPI photographs. The rainbands B_1-B_5 were similar in size and rainfall intensity. The average bandwidth was 48 km and the mean rainfall rate 1.6 mm h^{-1} (peak rainfall rates due to each rainband ranged from 5 to 8 mm h^{-1}). The mean bandwidth and rainfall rate of B_6 were 100 km and 3.6 mm h^{-1}, respectively, the peak rainfall rate due to B_6 was 14 mm h^{-1}. The mean speed of motion of the rainbands was about 35 km h^{-1}. A systematic change of orientation of the rainbands, from north-south to northwest-southeast then back to north-south direction, was observed. Rainbands B_1 and B_2 occurred toward the leading edge of the large-scale frontal system and their orientation was similar to bands on the leading edge side of an occluded frontal system studied by Kreitzberg and Brown (1970). Bands B_3 and B_4 occurred in the warm sector of a weak low pressure system that developed on the cold front of the occluded system, and they may have been parallel to the cold front in the developing wave, although this could not be demonstrated conclusively. Bands B_5 and B_6 were definitely parallel to the cold front.

Small-scale elements observed on the radar PPI were embedded in the rainbands. These elements had similar mean dimensions (~244 km² and 47 km² for radar echo level-0 and level-4, respectively) and spatial concentration (~1.1 and 4.0 per 1000 km² for level-0 and level-4 echo, respectively) as those of "small mesoscale areas" and "cells" observed by Austin and Houze (1972) in New England. The motion of the small-scale elements was closely related to the wind in the 850 to 700 mb layer (Fig 9), which was probably the region of generation of precipitation particles. Browning and Harrold (1969), Austin and Houze (1972), and Harrold (1973) also found that small-scale elements were steered by the winds in the mid-troposphere. However, in their cases the steering level appeared to be between 700 and 500 mb. The motion of the larger rainbands in the present study was not obviously related to the wind field, their motion may have been controlled by some other factors such as frontal motion.

Much of the precipitation in this storm was due to small mesoscale rainfall areas (~60 km in horizontal dimension), which were not embedded within any of major rainbands B_1-B_6. These mesoscale areas also moved with the wind between 850 and 700 mb.

The vertical extent of the mesoscale rainfall areas was estimated to range from 3 to 7 km, which is close to the average vertical extent of rainfall areas in extra-tropical cyclones observed by Austin and Houze (1972) and Browning and Harrold (1969).

A particularly interesting feature was the rainfall peak labelled C_7 in Fig. 5c. This was purely a local phenomenon produced by the local convergence of airflow and associated lifting and release of potential instability (Fig. 5b) after the passage of primary cold front which produced significant convective motions that penetrated through a layer of dry air aloft (Fig. 5a). This convection was responsible for the occurence of the intense precipitation. This mesoscale feature (C_7) did not exhibit any motion, and in this respect was distinctly different from all of the other mesoscale areas.

Acknowledgments

The author wishes to express his most sincere appreciation to Professor Robert A. Houze for his guidance, encouragement and critical comments during the course of this study.

Special thanks go to Professor Richard J. Reed and Professor Peter V. Hobbs for their suggestions and reading the manuscript.

Appreciation is also expressed to Mr. K. Biswas for his help in preparation of data and discussion.

This study was supported by the National Science Council, Republic of China.

References

Austin, P. M., and R. A. Houze, 1972: Analysis of the structure of precipitation pattern in New England. *J. Appl. Meteor.*, 11, 926-935.

Browning, K.A., 1974: Mesoscale structure of rain systems in the British Isles. *J. Meteor, Soc. Japan*, 50, 314-327.

_____and T.W. Harrold, 1969: Air motion and precipitation growth in a wave depression. *Quart. J. Roy. Meteor Soc.*, 95, 288-309.

_____M.E. Hardman, T.W. Harrold and C. W. Pardoe, 1972: The structure of rainbands within a mid-latitude depression. *Quart. J. Roy. Meteor. Soc*, 99, 215-231.

Elliott, R. D., and E. L. Hovind, 1964: On convection bands within Pacific coast storms and their relation to storm structure. *J. Appl. Meteor.*, 3, 143-154.

Harrold, T.W., 1973: Mechanisms influencing the distribution of precipitation within baroclinic

disturbances. *Quart. J. [Roy. Meteor. Soc.*, 99, 232-251.

Houze, R. A., 1969: Characteristics of mesoscale precipitation areas. S. M. Thesis, Dept. of Meteorology, Massachusetts Institute of Technology, Cambridge, Mass., 77 pp.

Kreitzberg, C. W. and H. A. Brown, 1970: Mesoscale weather systems within an occlusion. *J. Appl. Meteor.*, 9, 417-432,

Nozumi, Y. and H. Arakawa, 1968: Pre-frontal rainbands in the warm sector of subtropical cyclones over the ocean. *J. Geophys Res.*, 73, 487-492.

Reed, R. W., 1972: Characteristics and development of mesoscale precipitation areas in extra-tropical cyclones. S. M. Thesis, Dept. of Meteorology, Massachusetts Institute of Technology, Cambridge, Mass, 94 pp

囚錮鋒面系統之中範圍降水型態

謝 信 良

中 央 象 氣 局

摘 要

本文係分析 1973 年 12 月 5～7 日通過美國華盛頓州之鋒面系統內的中範圍降水特性。利用自動雨量計及雷達資料，發現在鋒面過境期間有六個中範圍雨帶通過觀測網，其中前五個雨帶之寬度相仿，平均約 50 公里，第六個雨帶的寬度則較其他五個寬一倍。首二個雨帶出現於 12 月 5 日，其走向平行於囚錮鋒面系統之暖鋒，次二個雨帶出現於 6 日，是發生在沿原來冷鋒上新生波動的暖區內，它們的走向似與冷鋒一致，最後二個雨帶是件隨主要冷鋒出現於 7 日，且與之平行。在雨帶內之較小範圍雨區的集中度由雷達回波上顯示約爲每一千平方公里一至三個，平均大小在 50 至 240 平方公里之間，此諸回波隨着 850-700mb 之高空風移動，而雨帶本身之移動方向似與 500mb 高空風之關係較密切。至於雨區之垂直伸展高度則約爲 3 至 7 公里。